

## Supporting Information

### Nitrogen-doped carbon quantum dots for fluorescence sensing, anti-counterfeiting and logic gate operation

Li Xu,<sup>a</sup> Yi Qian,<sup>a</sup> Lei Bao,<sup>a</sup> Wei Wang,<sup>a</sup> Nengmei Deng,<sup>a</sup> Li Zhang,<sup>a</sup> Guanglin Wang,<sup>a</sup> Xucheng Fu,<sup>\*a</sup> Wei Fu<sup>\*a</sup>

<sup>a</sup> Key Laboratory of Biomimetic Sensor and Detecting Technology of Anhui Province, West Anhui University, Lu'an 237012, China.

\* Corresponding author:

*E-mail address:* fxc8307@wxc.edu.cn; w-fu17@tsinghua.org.cn

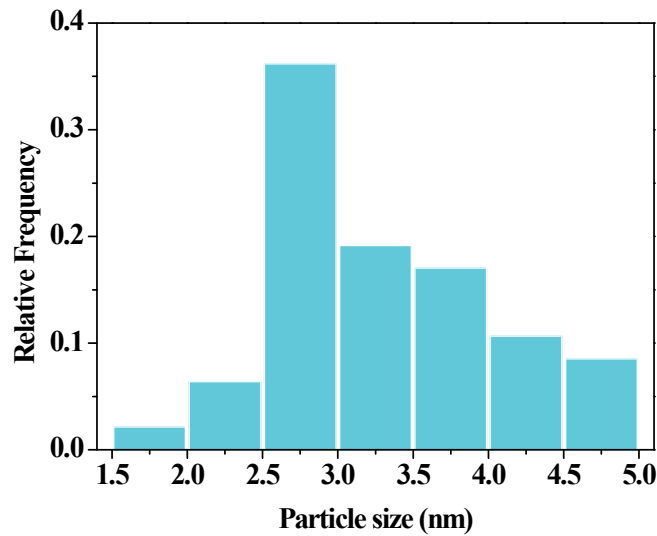


**Fig. S1** Average particle size of N-CQDs ( $3.27 \pm 0.69$  nm)

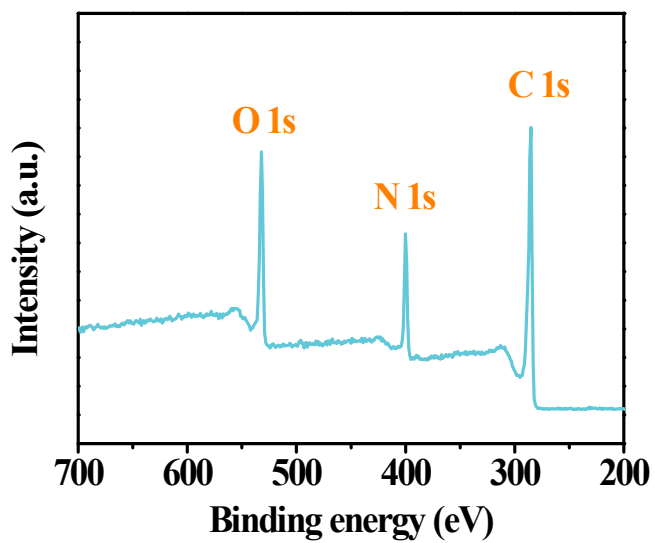


**Fig. S2** XPS survey spectrum of N-CQDs

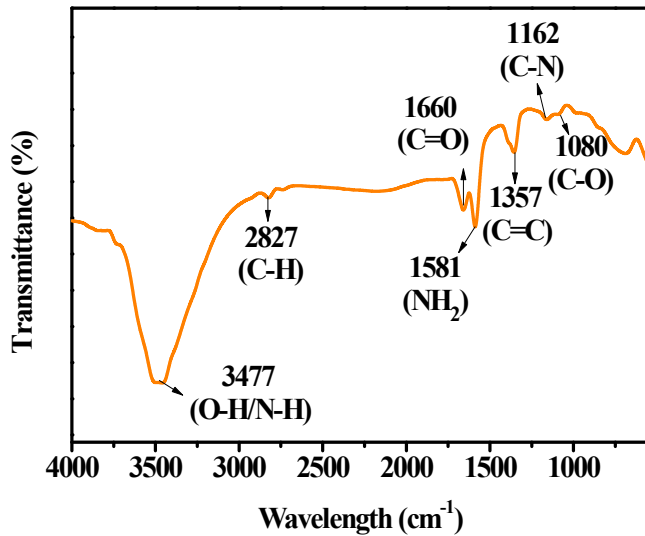


**Fig. S3** FT-IR spectrum of N-CQDs

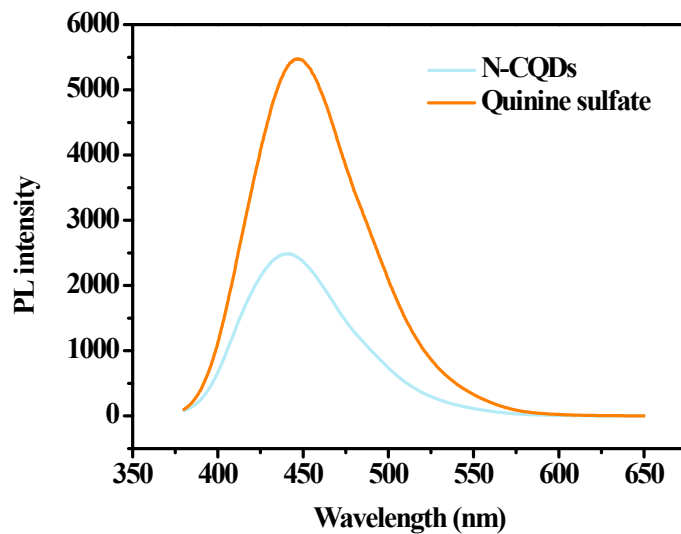


**Fig. S4** PL spectrum of N-CQDs and quinine sulfate

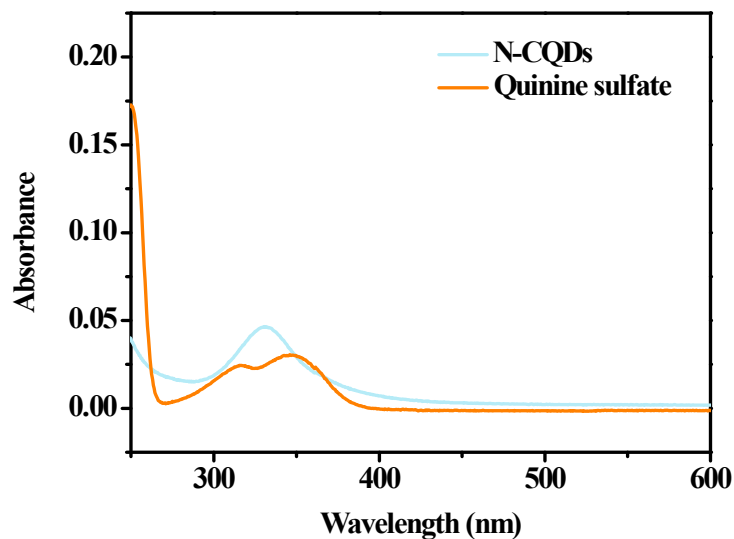


**Fig. S5** UV-vis spectrum of N-CQDs and quinine sulfate

**Table S1. Quantum yield of the N-CQDs**

Sample	Abs. at 360nm	PL Integrated intensity	Refractive index of solvent (n)	PLQY (%)
Quinine sulfate	0.0298	448518.3	1.33	54
N-CQDs	0.0292	196834.1	1.33	25.9

**Table S2** Comparison of the fluorescence quantum yield (QY) of CQDs.

Quantum dots	QY (%)	References
Nitrogen-doped carbon quantum dots (N-CQDs)	18	[1]
N-doped carbon quantum dots (N-CQDs)	21.9	[2]
Boron-nitrogen co-doped carbon quantum dots (B, N-CQDs)	14.5	[3]
Nitrogen modified carbon quantum dots (N-CQDs)	16.8	[4]
Nitrogen doped carbon quantum dot (N-CQDs)	14.81	[5]
Nitrogen-rich carbon quantum dots (N-CQDs)	25	[6]
Nitrogen doped carbon quantum dots (N-CQDs)	12.33	[7]
Nitrogen-doped carbon quantum dots (N-CQDs)	17.5	[8]
Nitrogen-doped carbon quantum dots (N-CQDs)	22.14	[9]
N-doped carbon quantum dots (CQDs)	9	[10]
Nitrogen, phosphorus codoped carbon quantum dots (N, P-CQDs)	21.7	[11]
N-CQDs	25.9	This work

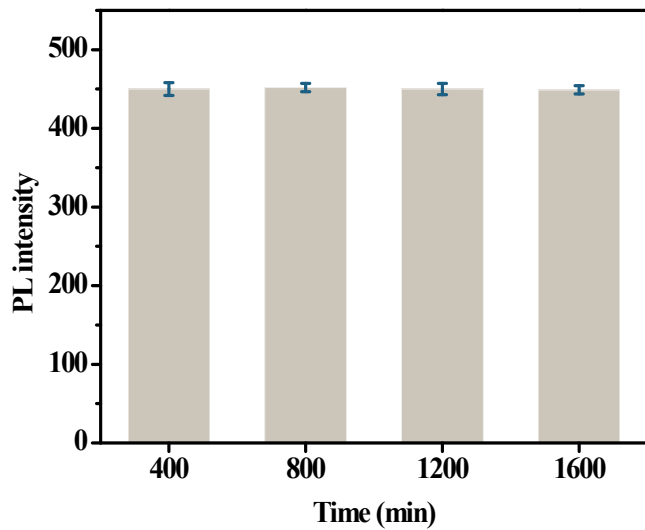


**Fig. S6** Stability testing of N-CQDs



**Fig. S7** Fluorescence photos of different metal ions detected by N-CQDs

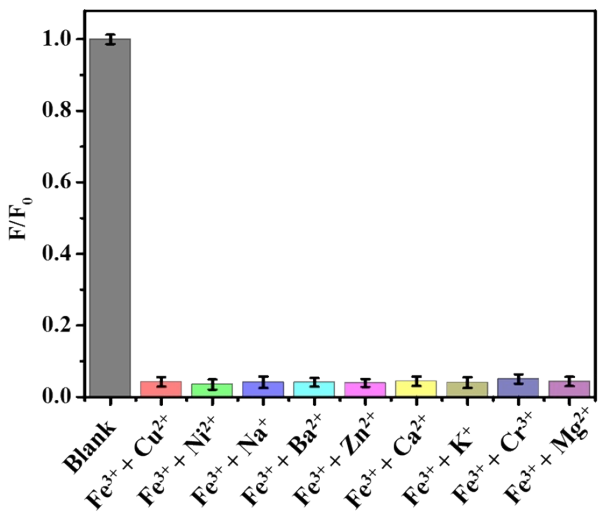


**Fig. S8** Interference diagram for  $\text{Fe}^{3+}$  detection. The  $\text{Fe}^{3+}$  concentration is 100  $\mu\text{M}$ , and the other ions are 300  $\mu\text{M}$ .

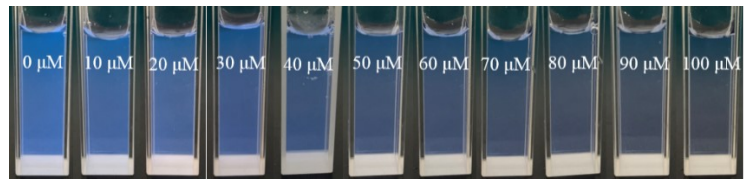


**Fig. S9** Fluorescence photos of N-CQDs detecting different concentrations of  $\text{Fe}^{3+}$

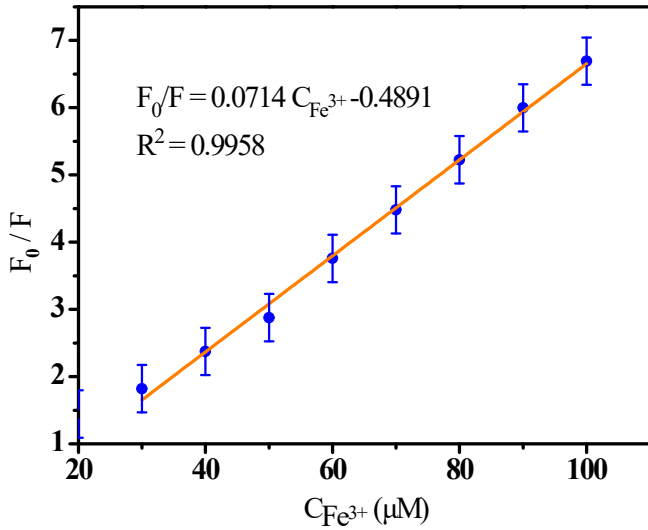


**Fig. S10** Linear relationship of fluorescence intensity as a function of  $\text{Fe}^{3+}$  concentration in the range of 30–100  $\mu\text{M}$ .

**Table S3.** Fe<sup>3+</sup> sensing properties with different fluorescent probes. Limit of detection LOD = 3σ/K (where σ is the standard deviation of the blank sample and K is the slope of the linear equation).

Fluorescent probes	Synthesis Method	Excitation/Emission wavelength	Quantum yield	LOD	References
Carbon quantum dots (CQDs)	Hydrothermal method	340/420 nm	22.7 %	0.2 μM.	[12]
Mopan persimmons derived carbon quantum dots (MP-CQDs)	Hydrothermal method	376/458 nm	8.39 %	0.324 μM	[13]
Nitrogen-doped carbon quantum dots (N-CQDs)	Hydrothermal method	350/425 nm	22 %	3 μM	[14]
Carbon quantum dots (CQDs)	Hydrothermal method	340/476 nm	23.68 %	0.77 μM	[15]
Phosphorus-doped carbon quantum dots (N, P-CQDs)	Hydrothermal method	320/425 nm	17.74 %	0.447 μM	[16]
Carbon quantum dot (CQDs)	Hydrothermal method	330/400 nm	18.1 %	4 μM	[17]
N-CQDs	Solvothermal method	340/442 nm	25.9 %	0.28 μM	This work

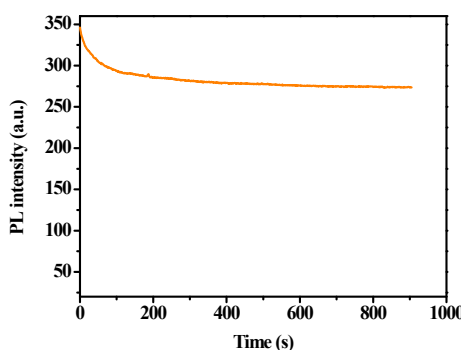


**Fig. S11** Time dependent fluorescence graph after adding Fe<sup>3+</sup>

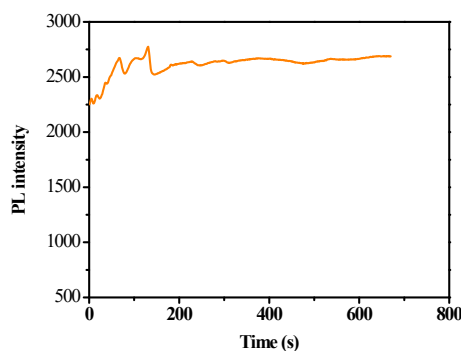


**Fig. S12** Time dependent fluorescence graph after adding AA

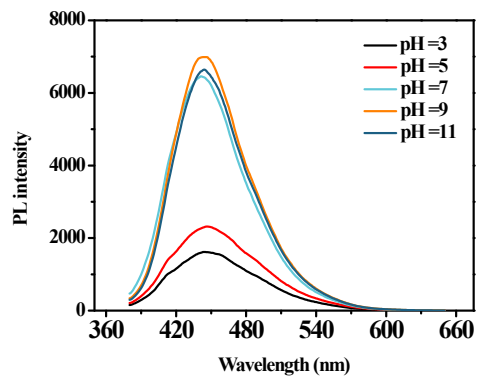


**Fig. S13** The fluorescence intensity of N-CQDs as a function of pH Values

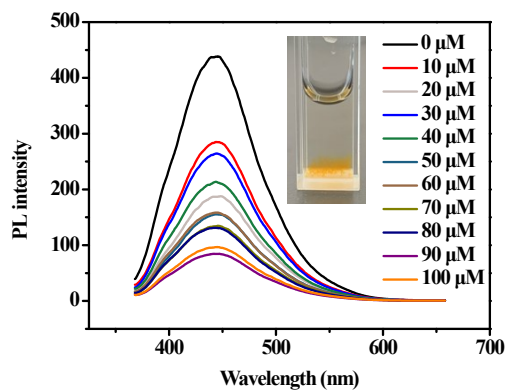


**Fig. S14** Detection of  $\text{Fe}^{3+}$  in a solution with pH=9.18, brown precipitates appeared at the bottom of the cuvette (inset)

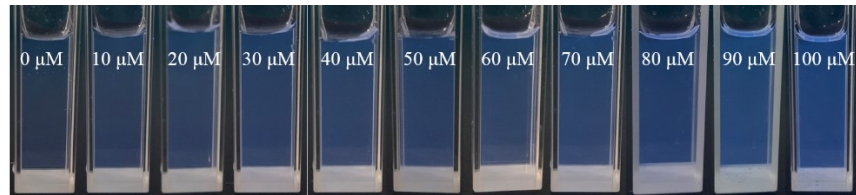


**Fig. S15** Fluorescence photos of N-CQDs/ $\text{Fe}^{3+}$  detecting different concentrations of AA

**Table S4.** AA sensing properties with different fluorescent probes. Limit of detection LOD =  $3\sigma/K$  (where  $\sigma$  is the standard deviation of the blank sample and  $K$  is the slope of the linear equation).

Fluorescent probes	Linear range ( $\mu\text{mol/L}$ )	Applications	LOD	Reference s
N,S co-doped carbon dots (N,S-CDs)-Fe <sup>3+</sup>	10-200	Fruits	4.69 $\mu\text{M}$ .	[18]
Nitrogen, phosphorus co-doped carbon quantum dots (N, P-CQDs)-Fe <sup>3+</sup>	1-200	Fruits	0.84 $\mu\text{M}$	[19]
Red-carbon quantum dots (R-CQDs)-Fe <sup>3+</sup>	1-50	Human body fluids and vitamin C tablets	0.42 $\mu\text{M}$	[20]
Nitrogen-doped carbon quantum dots (N-CQDs)-Fe <sup>3+</sup>	10-100	Medical tablet	1.8 $\mu\text{M}$	[21]
Cobalt-doped carbon quantum dots (Co-CQDs)-Fe <sup>3+</sup>	10-400	Fruits	0.27 $\mu\text{M}$	[22]
Carbon quantum dots (CQDs)-Fe <sup>3+</sup>	0-350	Human biological samples	5.34 $\mu\text{M}$	[23]
N-CQDs-Fe <sup>3+</sup>	30-90	Fruits	0.81 $\mu\text{M}$	This work



**Fig. S16** Fluorescence photos of different substances detected by N-CQDs/Fe<sup>3+</sup>

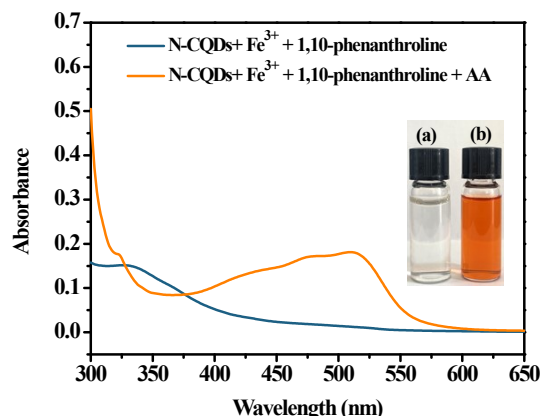


**Fig. S17** UV-vis absorption spectra of the N-CQDs + Fe<sup>3+</sup> + 1,10-phenanthroline and the N-CQDs + Fe<sup>3+</sup> + 1,10-phenanthroline + AA. Inset: Photographs of solutions (a) N-CQDs + Fe<sup>3+</sup> + 1,10-phenanthroline and (b) N-CQDs + Fe<sup>3+</sup> + 1,10-phenanthroline + AA (b) under daylight.

## References

- 1 B. K. John, N. John, B. K. Korah, C. Thara, T. Abraham and B. Mathew, *J. Photoch. Photobio. A*, 2022, **432**, 114060.
- 2 C. Yu, D. Qin, X. Jiang, X. Zheng and B. Deng, *J. Pharmaceut. Biomed.*, 2021, **192**, 113673.
- 3 C. Wang, Q. Sun, C. Li, D. Tang, H. Shi, E. Liu, P. Guo, W. Xue and J. Fan, *Mater. Res. Bull.*, 2022, **155**, 111970.
- 4 R. Chen, Z. Xing, Y. Lu, S. Li, J. Song, X. Zhang and R. Zhang, *Opt. Mater.*, 2022, **131**, 112630.
- 5 S. Patel, K. Shrivastava, D. Sinha, I. Karbhal and T. K. Patle, *Spectrochim. Acta A*, 2023, **299**, 122824.
- 6 H. Ren, M. Li, Y. Liu, T. Zhao, R. Zhang and E. Duan, *Sci. Total Environ.*, 2022, **811**, 152389.
- 7 S. Ding, P. Tan, J. Wen, T. Li and W. Wang, *Sci. Total Environ.*, 2022, **814**, 152745.
- 8 T. Y. Shen, P. Y. Jia, D. S. Chen and L. N. Wang, *Spectrochim. Acta A*, 2021, **248**, 119282.
- 9 G. Wang, S. Zhang, J. Cui, W. Gao, X. Rong, Y. Lu and C. Gao, *Anal. Chim. Acta*, 2022, **1195**, 339478.
- 10 Z. Zhai, J. Xu, T. Gong, B. Cao, K. Cui, L. Hou and C. Yuan, *Inorg. Chem. Commun.*, 2022, **140**, 109387.
- 11 X. Li, C. Wang, P. Li, X. Sun, Z. Shao, J. Xia, Q. Liu, F. Shen and Y. Fang, *Food Chem.*, 2023, **409**, 135243.
- 12 U. Latief, S. U. Islam, Z. M. S.H. Khan and M. S. Khan, *Spectrochim. Acta A*, 2021, **262**, 120132.
- 13 H. Ma, L. Guan, M. Chen, Y. Zhang, Y. Wu, Z. Liu, D. Wang, F. Wang and X. Li, *Chem. Eng. J.*, 2023, **453**, 139906.
- 14 L. Gu, J. Zhang, G. Yang, Y. Tang, X. Zhang, X. Huang, W. Zhai, E. K. Fodjo and C. Kong, *Food Chem.*, 2022, **376**, 131898.
- 15 L. Zhu, D. Shen, Q. Liu, C. Wu and S. Gu, *Appl. Surf. Sci.*, 2021, **565**, 150526.
- 16 S. R. Zhang, S. K. Cai, G. Q. Wang, J. Z. Cui and C. Z. Gao, *J. Mol. Struct.*, 2021, **1246**, 131173.
- 17 H. Ren, F. Qi, A. Labidi, A. A. Allam, J. S. Ajarem, D.W. Bahnemann and C. Wang, *ACS EST. Engg.*, 2022, **3**, 260-270.
- 18 X. Luo, W. Zhang, Y. Han, X. Chen, L. Zhu, W. Tang, J. Wang, T. Yue and Z. Li, *Food Chem.*, 2018, **258**, 214-221.
- 19 X. Li, C. Wang, P. Li, X. Sun, Z. Shao, J. Xia, Q. Liu, F. Shen and Y. Fang, *Food Chem.*, 2023, **409**, 135243.
- 20 S. Huang, B. Li, G. Ning, W. Zhang, P. Mu, S. Chen and Q. Xiao, *Anal. Methods*, 2023, **15**, 3101-3113.

- 21 L. Gu, J. Zhang, G. Yang, Y. Tang, X. Zhang, X. Huang, W. Zhai, E. K. Fodjo and C. Kong, *Food Chem.*, 2022, **376**, 131898.
- 22 C. Li, J. Zeng, D. Guo, L. Liu, L. Xiong, X. Luo, Z. Hu and F. Wu, *ACS Appl. Mater. Interfaces*, 2021, **13**, 49453-49461.
- 23 X. Gao, X. Zhou, Y. Ma, T. Qian, C. Wang and F. Chu, *Appl. Surf. Sci.*, 2019, **469**, 911-916.